Electronic supplementary information (ESI)

Impact of Fluorine Substitution Position on Triarylamine-Based Hole Transport Materials in Perovskite Solar Cells

Bhim Raju Telugu,*[a] Hanbo Jung,[ab] Zhanglin Guo,[abc] Toshinori Matsushima*[abcd]

[a)] *International Institute for Carbon-Neutral Energy Research (WPI-I2CNER), Kyushu University, Fukuoka 819-0395, Japan. E-mail: tmatusim@i2cner.kyushu-u.ac.jp*

[b)] *Center for Energy Systems Design (CESD), International Institute for Carbon-Neutral Energy Research (WPI-I2CNER), Kyushu University, Fukuoka 819-0395, Japan*

[c)] *Department of Automotive Science, Graduates School of Integrated Frontier Sciences, Kyushu University, 744 Motooka, Nishi, Fukuoka 819-0395, Japan*

[d)] *Department of Applied Chemistry, Faculty of Engineering, Kyushu University, Fukuoka 819-0395, Japan.*

*Corresponding authors: Telugu Bhim Raju, Toshinori Matsushima,

Email: tmatusim@i2cner.kyushu-u.ac.jp

Email: bhimraju@i2cner.kyushu-u.ac.jp

1. Experimental section

1.1. Materials and methods.

All solvents and reagents were purchased from Aldrich, TCI, or Wako and used as received with a stated purity above 98%. Thin-layer chromatography (TLC) was performed on Merck KGaA precoated silica gel 60F254 aluminum sheets. Column chromatography was carried out using glass columns packed with Silicycle Ultra Pure Silica Flash P60 silica gel (40–63 μm, 230–400 mesh). Unless otherwise noted, all reactions and manipulations were conducted under a nitrogen atmosphere. Reagent-grade solvents were used for synthesis, whereas spectroscopy-grade solvents were employed for spectroscopic measurements. All solvents were dried using standard procedures prior to use.

1.2. Characterizations

^{1}H and ^{13}C NMR spectra were recorded on a Bruker AVANCE III 600 MHz spectrometer in deuterated chloroform ($CDCl_3$), using tetramethylsilane (TMS) as the internal standard. Chemical shifts were referenced to the residual solvent peaks (δ = 7.26 ppm for ^{1}H and δ = 77.23 ppm for ^{13}C). All spectra were obtained at room temperature, with chemical shifts reported in ppm and coupling constants in Hz. Mass spectrometric analysis was conducted using an ultra-performance liquid chromatography time-of-flight mass spectrometer (UPLC-TOF-MS, Agilent 1290–6545). The corresponding NMR and mass spectra are presented in Figures S2–S25. UV–Vis–NIR absorption spectra were measured for both solution-state (chloroform) and thin-film samples (on quartz substrates) using a Jasco V-730 spectrophotometer. Fluorescence spectra of the same samples were recorded using a Jasco FP-8300 fluorescence spectrophotometer. Cyclic voltammetry (CV) measurements were performed using a CHI 660A electrochemical workstation equipped with platinum electrodes and an Ag/AgCl reference electrode, operated at a scan rate of 50 mV s^{-1}. All CV experiments were carried out in a nitrogen-saturated solution of 0.1 M tetrabutylammonium hexafluorophosphate (Bu_4NPF_6) in dichloromethane (DCM; CH_2Cl_2). The ground-state geometries and vertical excitation energies of the synthesized HTM molecules were investigated computationally using density functional theory (DFT) and time-dependent DFT (TD-DFT) calculations, employing the B3LYP functional with the 6-31G(d,p) basis set. All calculations were performed in the gas phase (no solvent model applied) using the Gaussian 16 software package. Scanning electron microscopy (SEM) top-view images of the perovskite films were obtained using a field-emission SEM system (JSM-7900F, JEOL) operated at an acceleration voltage of 5 kV with a magnification of ×10,000. Thermal gravimetry-differential

thermal analysis (TG-DTA; 2400SA, Bruker) was carried out, with a heating rate of 10°C min^{-1} under a nitrogen atmosphere.

1.3 Synthetic procedure

The synthetic routes of the HTMs are illustrated in Figure S1, with detailed procedures provided. All intermediates, including 4-bromo-3-fluoro-*N*,*N*-bis(4-methoxyphenyl)aniline, 4-bromo-2-fluoro-*N*,*N*-bis(4-methoxyphenyl)aniline, and *N*-(2-fluorophenyl)-*N*-(4-methoxyphenyl)-9,9-dimethyl-9H-fluoren-2-amine, were synthesized via the Buchwald–Hartwig amination method.[S1,S2] The target HTMs were subsequently prepared through palladium-catalyzed Suzuki–Miyaura coupling reactions using tetrakis(triphenylphosphine)palladium(0) ($Pd(PPh_3)_4$) as the catalyst. [S3,S4]

3.1 synthesis scheme:

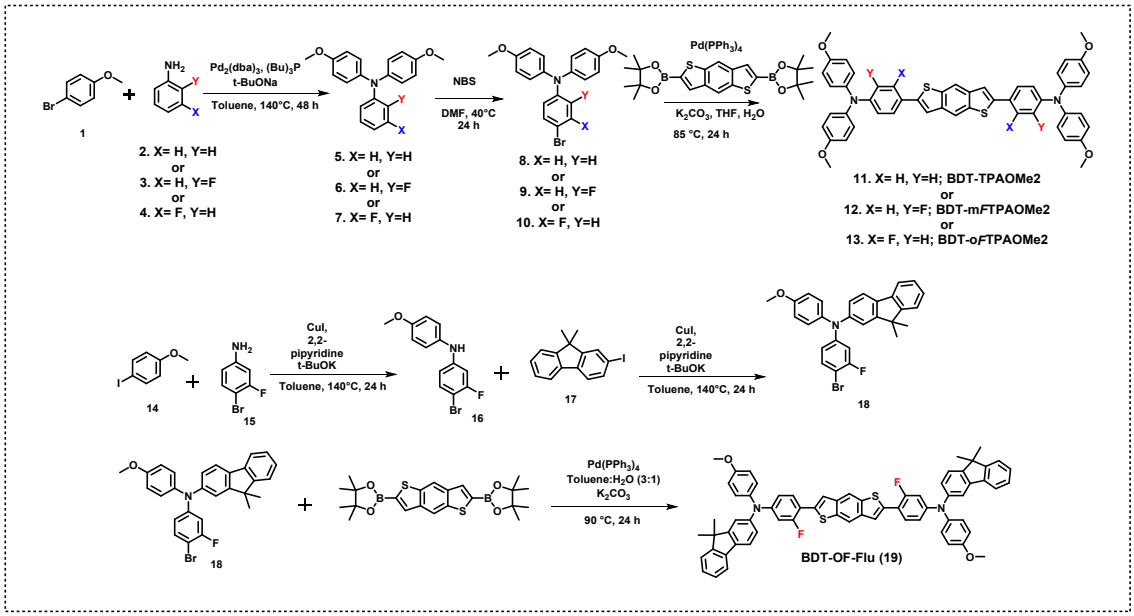

Fig. S1. Synthetic route for HTMs.

General synthesis procedure for compounds 6 and 7

A solution of aniline (9.85 mmol), 4-bromothioanisole (29.54 mmol), t-BuONa (39.39 mmol), and $P(t\text{-}Bu)_3$ (2.00 mmol) in dry toluene (50 mL) was degassed with nitrogen for 30 min. $Pd(OAc)_2$ (220 mg, 0.98 mmol) was then added under a nitrogen atmosphere, and the resulting mixture was refluxed for 48 h. After cooling to room temperature, the crude product was extracted

with chloroform and washed with water. Compounds 6 and 7 were obtained as a brown solid after purification by column chromatography (hexane/chloroform, 2:1, v/v).

2-fluoro-N,N-bis(4-methoxyphenyl)aniline (6)

^{1}H NMR (600 MHz, $CDCl_3$) δ 7.48 (s, 4H), 7.29 (d, J = 11.7 Hz, 10H), 7.16 (d, J = 8.5 Hz, 15H), 7.02 (d, J = 8.4 Hz, 15H), 4.01 (s, 22H); ^{13}C NMR (126 MHz, $CDCl_3$) δ 158.63, 156.64, 155.34, 141.49, 135.71, 127.92, 124.74, 124.05, 117.05, 114.60, 77.41, 77.16, 76.91, 55.64. Yield- 72%.

Compound 7

^{1}H NMR (600 MHz, $CDCl_3$) δ 7.29 (d, J = 8.7 Hz, 4H), 7.06 (d, J = 8.7 Hz, 4H), 6.87 (d, J = 8.2 Hz, 1H), 6.81 (d, J = 11.8 Hz, 1H), 6.71 (t, J = 7.8 Hz, 1H), 3.99 (s, 6H); ^{13}C NMR (151 MHz, $CDCl_3$) δ 164.37, 162.76, 156.38, 150.68, 148.62, 140.26, 129.90, 127.17, 125.41, 115.31 – 114.76, 113.84, 106.62 – 106.24, 106.23, 77.37, 77.16, 76.95, 55.43. Yield- 69%.

General synthesis procedure for compounds 9 and 10

To a solution of compound 9 or 10 (2.73 mmol) in DMF (30 mL), NBS (3.00 mmol) was added at 0 °C. The reaction mixture was then warmed to room temperature and stirred at 40 °C for 12 h in the dark. The reaction was quenched with water and extracted with chloroform. The organic layer was dried, and the solvent was removed under reduced pressure. The crude product was purified by column chromatography (hexane/chloroform, 2:1, v/v) to afford compound 9 or 10 as a pale green viscous oil.

4-bromo-2-fluoro-N,N-bis(4-methoxyphenyl)aniline (9)

^{1}H NMR (600 MHz, $CDCl_3$) δ 7.21 (d, J = 10.6 Hz, 1H), 7.14 (d, J = 8.8 Hz, 1H), 6.92 (d, J = 8.4 Hz, 4H), 6.79 (d, J = 8.4 Hz, 4H), 3.78 (s, 6H); ^{13}C NMR (126 MHz, $CDCl_3$) δ 155.68, 141.00, 128.42, 128.03, 124.31, 120.68, 115.70, 114.72, 55.65. Yield- 90%.

4-bromo-3-fluoro-N,N-bis(4-methoxyphenyl)aniline (10)

^{1}H NMR (600 MHz, $CDCl_3$) δ 7.26 – 7.20 (m, 4H), 7.10 (d, J = 8.6 Hz, 12H), 6.88 (d, J = 8.7 Hz, 12H), 6.67 (d, J = 11.2 Hz, 3H), 6.58 (d, J = 8.7 Hz, 3H), 3.81 (s, 18H); ^{13}C NMR (151 MHz, $CDCl_3$) δ 156.66, 149.94, 139.68, 132.99, 127.25, 115.88, 114.98, 107.04, 106.87, 97.62, 97.48, 55.48. Yield- 85%.

General synthesis procedure for compounds 11, 12 and 13

2,6-Bis(4,4,5,5-tetramethyl-1,3,2-dioxaborolan-2-yl)benzo[1,2-b:4,5-b′]dithiophene (0.50 mmol) and compound 8–10 (656 mg, 1.42 mmol) were dissolved in tetrahydrofuran (15 mL, degassed with nitrogen), followed by the addition of $Pd(PPh_3)_4$ (0.06 mmol) and an aqueous K_2CO_3 solution (5 mL, 2.0 M, degassed with nitrogen). The mixture was refluxed for 24 h. After cooling to room temperature, the reaction mixture was extracted with dichloromethane and washed with water. The organic phase was dried, concentrated under reduced pressure, and the residue was purified by column chromatography (hexane/chloroform, 2:8, v/v) to afford compound 11, 12, or 13 as a yellow solid.

4,4'-(benzo[1,2-b:4,5-b']dithiophene-2,6-diyl)bis(N,N-bis(4-methoxyphenyl)aniline) (11)

^{1}H NMR (600 MHz, $CDCl_3$) δ 8.07 (s, 1H), 7.51 (d, J = 8.7 Hz, 2H), 7.39 (s, 1H), 7.15 – 7.05 (m, 4H), 6.95 (d, J = 8.7 Hz, 2H), 6.90 – 6.80 (m, 4H), 3.81 (s, 6H); ^{13}C NMR (151 MHz, $CDCl_3$) δ 156.25, 149.00, 144.40, 140.54, 138.60, 136.78, 127.12, 126.98, 126.19, 120.19, 116.78, 116.00, 114.88, 55.62. Yield- 67%.

4,4'-(benzo[1,2-b:4,5-b']dithiophene-2,6-diyl)bis(2-fluoro-N,N-bis(4-methoxyphenyl)aniline) (12)

^{1}H NMR (600 MHz, $CDCl_3$) δ 8.13 (s, 1H), 7.46 (s, 1H), 7.39 (dd, J = 23.6, 10.0 Hz, 2H), 7.07 (t, J = 7.8 Hz, 1H), 6.99 (d, J = 8.2 Hz, 4H), 6.83 (d, J = 8.2 Hz, 4H), 3.80 (s, 6H); ^{13}C NMR (151 MHz, $CDCl_3$) δ 157.70 (s), 156.04, 155.68, 143.18, 141.00, 138.64, 137.11, 135.86, 130.20, 127.14, 124.52, 122.74, 118.39, 116.56, 114.89, 114.65, 60.55, 55.62. Yield- 70%.

4,4'-(benzo[1,2-b:4,5-b']dithiophene-2,6-diyl)bis(3-fluoro-N,N-bis(4-methoxyphenyl)aniline) (13)

^{1}H NMR (600 MHz, $CDCl_3$) δ 8.12 (s, 1H), 7.58 (s, 1H), 7.44 (t, J = 8.7 Hz, 1H), 7.12 (d, J = 8.7 Hz, 4H), 6.88 (d, J = 8.7 Hz, 4H), 6.66 (dd, J = 20.0, 11.6 Hz, 2H), 3.82 (s, 6H); 13C NMR (151 MHz, $CDCl_3$) δ 161.25, 159.59, 156.82, 150.21, 139.65, 138.59, 138.22, 136.40, 129.51, 127.57, 120.36, 115.97, 115.03, 114.70, 113.38, 106.20, 106.02, 55.63. Yield- 73%.

Synthesis of 4-bromo-3-fluoro-N-(4-methoxyphenyl)aniline (16)

4-Bromo-3-fluoroaniline (2.00 g, 10.52 mmol), 4-iodoanisole (2.55 g, 10.52 mmol), CuI (0.20 g, 1.05 mmol), 2,2′-bipyridine (0.16 g, 1.05 mmol), and t-BuOK (1.50 g, 15.78 mmol) were added to dry toluene (100 mL) under a nitrogen atmosphere. The resulting mixture was refluxed for 48

h. After cooling to room temperature, the crude product was filtered and concentrated under reduced pressure. Compound 16 was obtained as a pale-yellow liquid after purification by column chromatography (hexane/chloroform, 1:2, v/v).

^{1}H NMR (600 MHz, $CDCl_3$) δ 7.28 (dd, J = 8.6, 8.0 Hz, 1H), 7.09 – 7.05 (m, 2H), 6.91 – 6.87 (m, 2H), 6.63 (dd, J = 11.0, 2.6 Hz, 1H), 6.53 – 6.49 (m, 1H), 5.57 (s, 1H), 3.81 (s, 3H). ^{13}C NMR (151 MHz, $CDCl_3$) δ 160.65, 159.03, 156.43, 146.96, 134.00, 133.58, 127.25, 123.95, 114.93, 112.01, 102.70, 102.53, 96.67, 96.53, 55.67. Yield- 65%, 2.0 gms.

Synthesis of N-(4-bromo-3-fluorophenyl)-N-(4-methoxyphenyl)-9,9-dimethyl-9H-fluoren-2-amine (18)

Compound 16 (3.00 g, 10.13 mmol), 2-iodo-9,9-dimethyl-9H-fluorene (3.24 g, 10.13 mmol), CuI (0.96 g, 5.06 mmol), 2,2′-bipyridine (0.78 g, 5.06 mmol), and t-BuOK (2.90 g, 30.39 mmol) were added to dry toluene (100 mL) under a nitrogen atmosphere. The reaction mixture was refluxed for 48 h. After cooling to room temperature, the crude product was filtered and concentrated under reduced pressure. Compound 18 was obtained as a pale-yellow solid after purification by column chromatography (hexane/chloroform, 1:2, v/v).

^{1}H NMR (600 MHz, $CDCl_3$) δ 7.66-7.65 (d, 1H), 7.61-7.58 (t, 1H), 7.41-7.40 (d, 1H), 7.34 – 7.25 (m, 3H), 7.19-7.17 (m, 1H), 7.16-7.12 (m, 2H), 7.04-7.03 (d, 1H), 6.90-6.88 (m, 2H), 6.81-6.61 (m, 2H), 3.83 (s, 3H), 1.43 (s, 6H). ^{13}C NMR (151 MHz, $CDCl_3$) δ 160.33, 158.70, 156.93, 156.67, 155.34, 155.20, 153.64, 150.33, 150.27, 149.63, 149.57, 146.95, 146.41, 139.80, 129.16, 128.36, 127.70, 127.69, 127.15, 122.63, 122.60, 120.88, 119.67, 118.77, 115.12, 115.0, 99.10, 55.60, 47.2, 27.19. Yield- 70%, 3.46 gms.

Synthesis of N-(4-(6-(4-((9,9-dimethyl-9H-fluoren-3-yl)(4-methoxyphenyl)amino)-3-fluorophenyl)benzo[1,2-b:4,5-b']dithiophen-2-yl)-2-fluorophenyl)-N-(4-methoxyphenyl)-9,9-dimethyl-9H-fluoren-2-amine (19)

2,6-Bis(4,4,5,5-tetramethyl-1,3,2-dioxaborolan-2-yl)benzo[1,2-b:4,5-b′]dithiophene (0.50 g, 1.13 mmol) and compound 18 (1.10 g, 2.26 mmol) were dissolved in tetrahydrofuran (15 mL, degassed with nitrogen), followed by the addition of $Pd(PPh_3)_4$ (0.063 g, 0.056 mmol) and an aqueous K_2CO_3 solution (5 mL, 2.0 M, degassed with nitrogen). The mixture was refluxed for 24 h. After cooling to room temperature, the reaction mixture was extracted with dichloromethane and washed with water. The organic phase was dried, concentrated under reduced pressure, and

the residue was purified by column chromatography (hexane/chloroform, 2:8, v/v) to afford compound 19 as an orange solid. Yield- 65%, 0.73 gms.

^{1}H NMR (600 MHz, $CDCl_3$) δ 8.14 (S, 1H), 7.66-7.61 (m, 3H), 7.50 (m, 1H), 7.41-7.40 (m, 1H), 7.33– 7.24 (m, 3H), 7.18-7.16 (m, 2H), 7.09-7.08 (m, 1H), 6.91-6.79 (m, 3H), 3.84 (s, 3H), 1.44 (s, 6H). ^{13}C NMR (151 MHz, $CDCl_3$) δ 159.57, 157.04, 155.35, 153.71, 149.81, 146.24, 139.67,138.85, 138.62, 136.47, 135.18, 129.59, 127.94, 127.16, 126.87, 123.85, 122.65, 120.90, 119.72, 119.14, 116.41, 116.09, 115.14, 55.64, 47.02, 27.22.

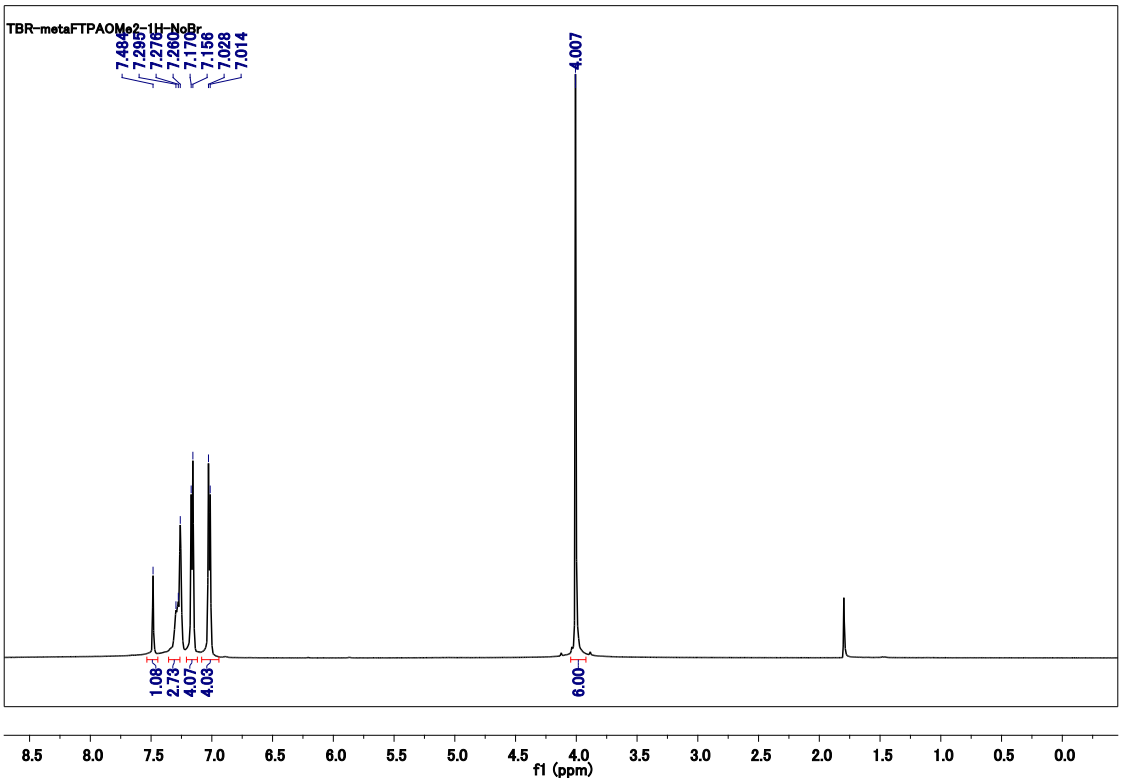

Fig. S2. ^{1}H NMR spectrum of compound 6 in deuterated chloroform.

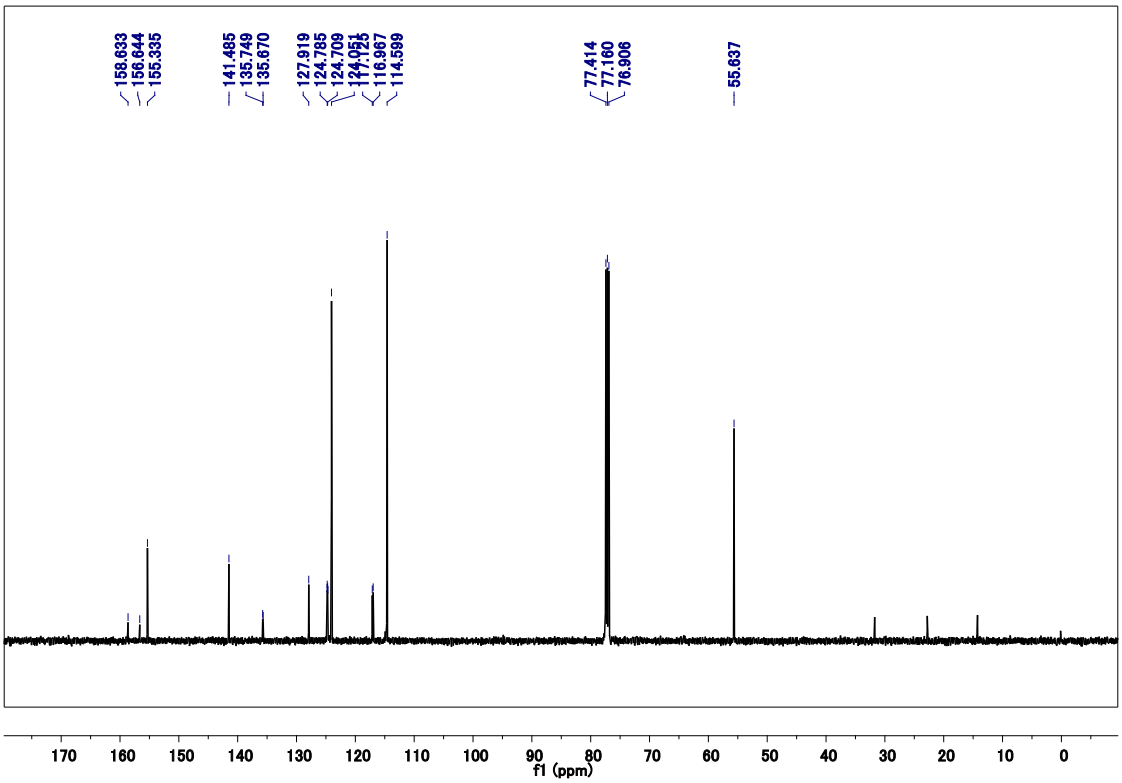

Fig. S3. ^{13}C NMR spectrum of compound 6 in deuterated chloroform.

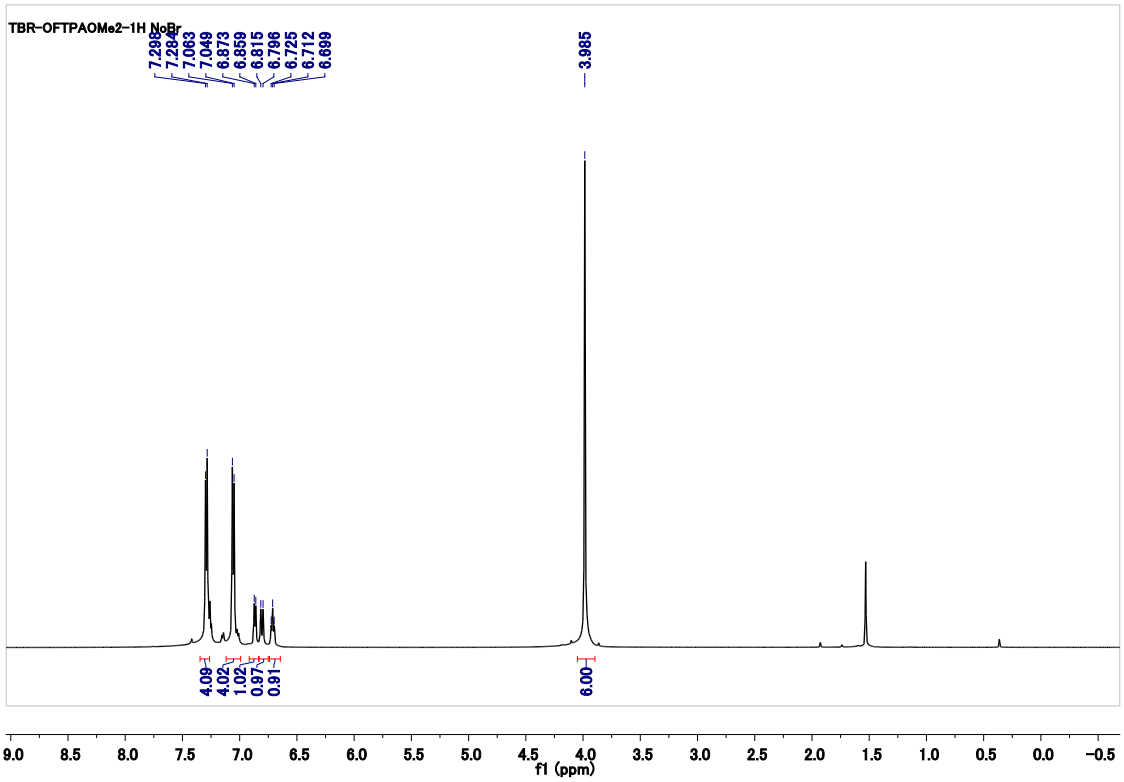

Fig. S4. ^{1}H NMR spectrum of compound 7 in deuterated chloroform.

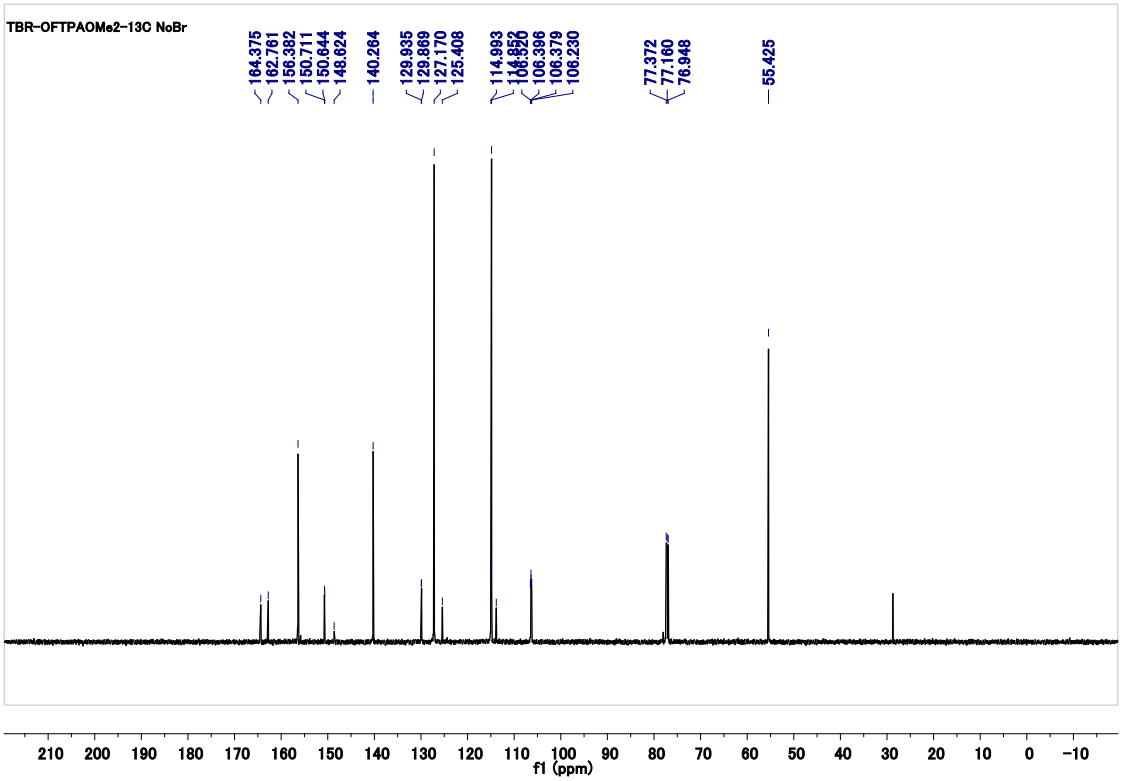

Fig. S5. ^{13}C NMR spectrum of compound 7 in deuterated chloroform.

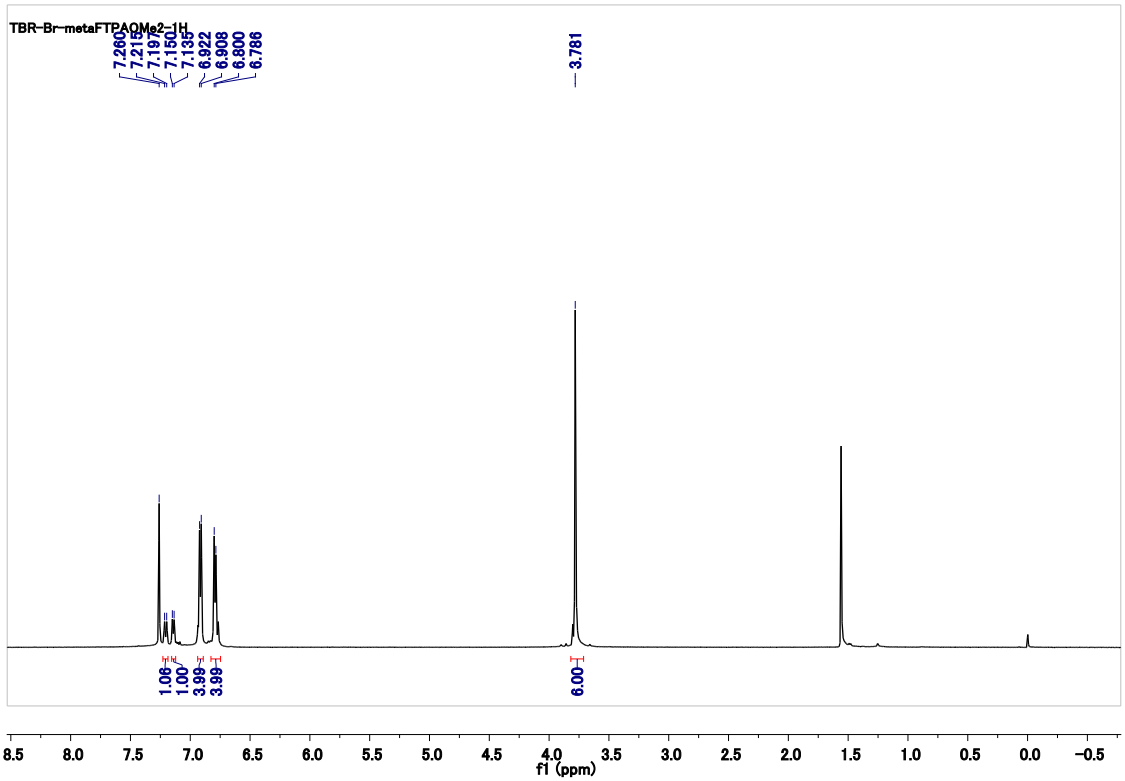

Fig. S6. ^{1}H NMR spectrum of compound 9 in deuterated chloroform.

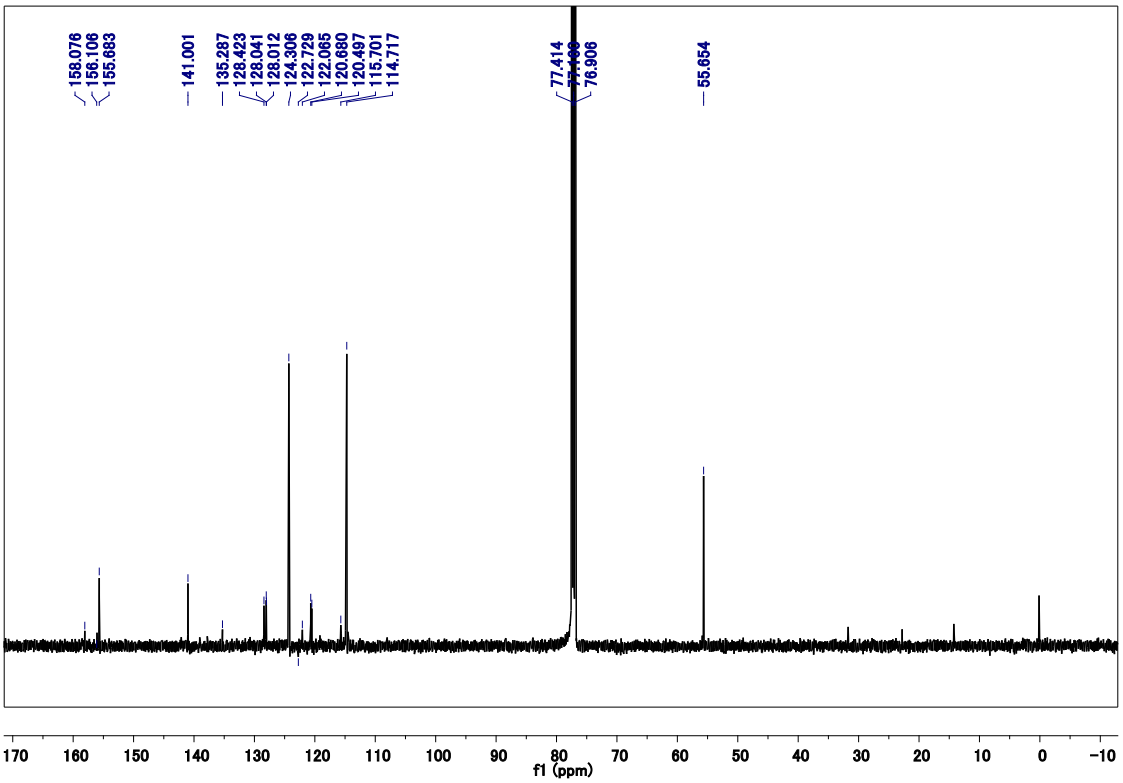

Fig. S7. ^{13}C NMR spectrum of compound 9 in deuterated chloroform.

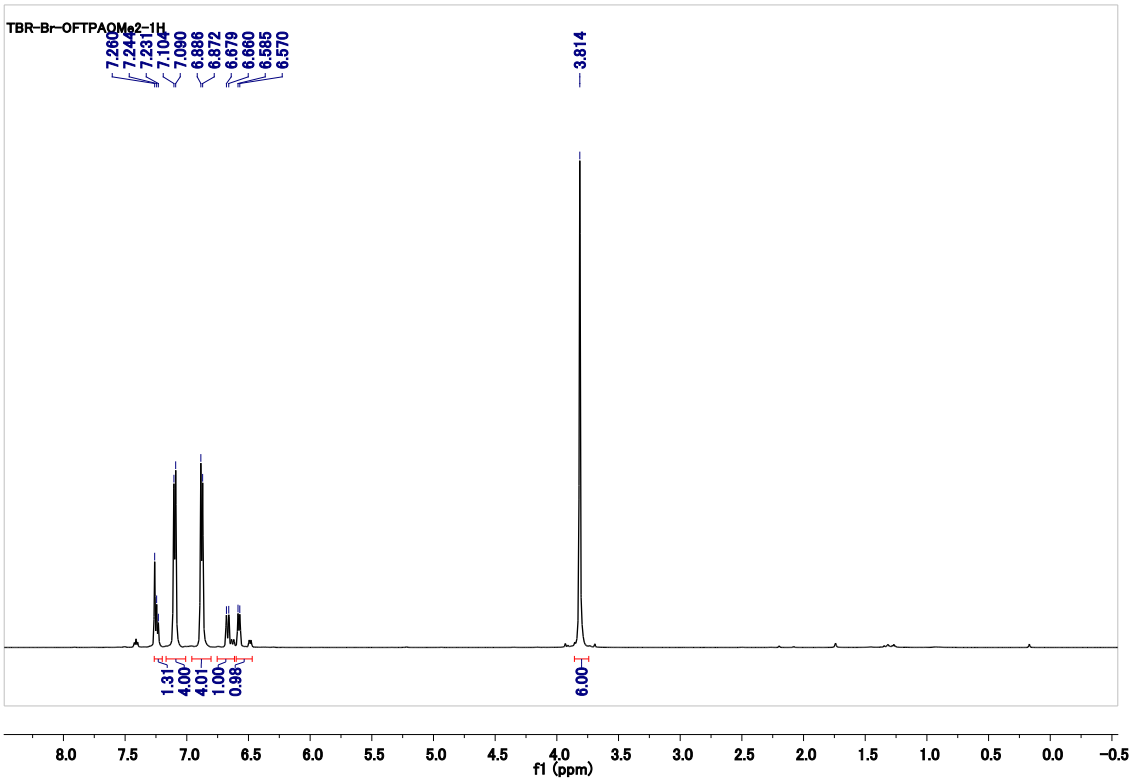

Fig. S8. ^{1}H NMR spectrum of compound 10 in deuterated chloroform.

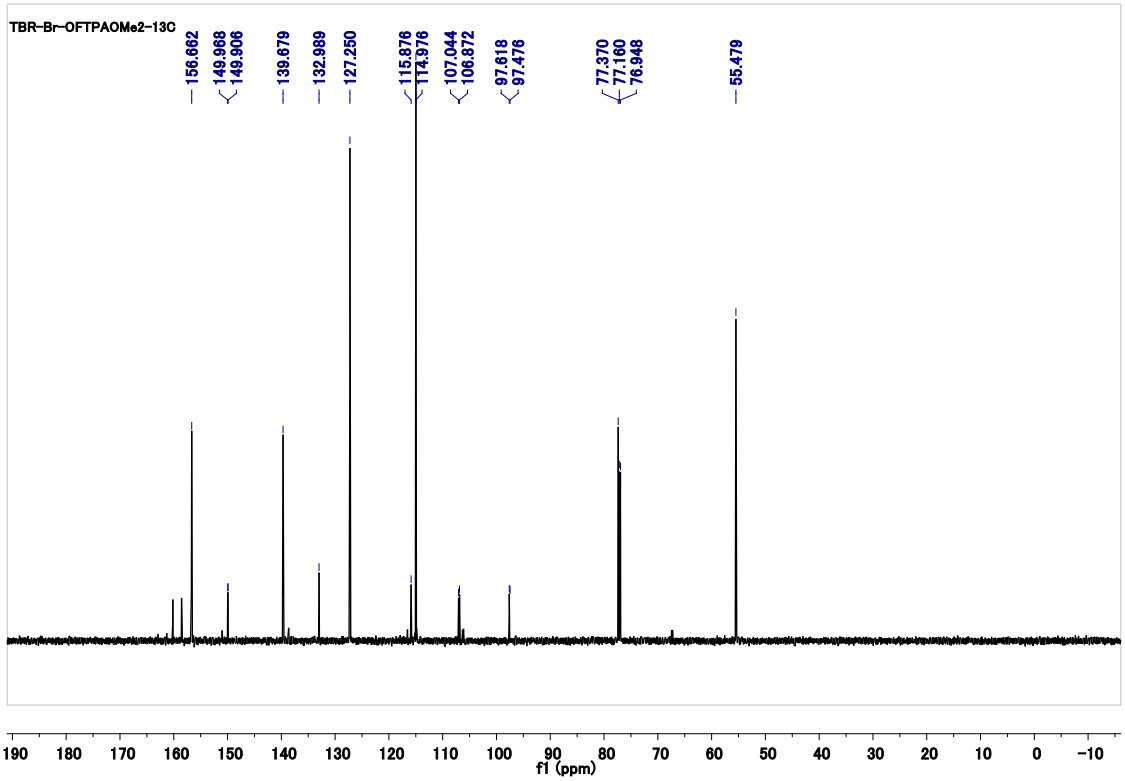

Fig. S9. ^{13}C NMR spectrum of compound 10 in deuterated chloroform.

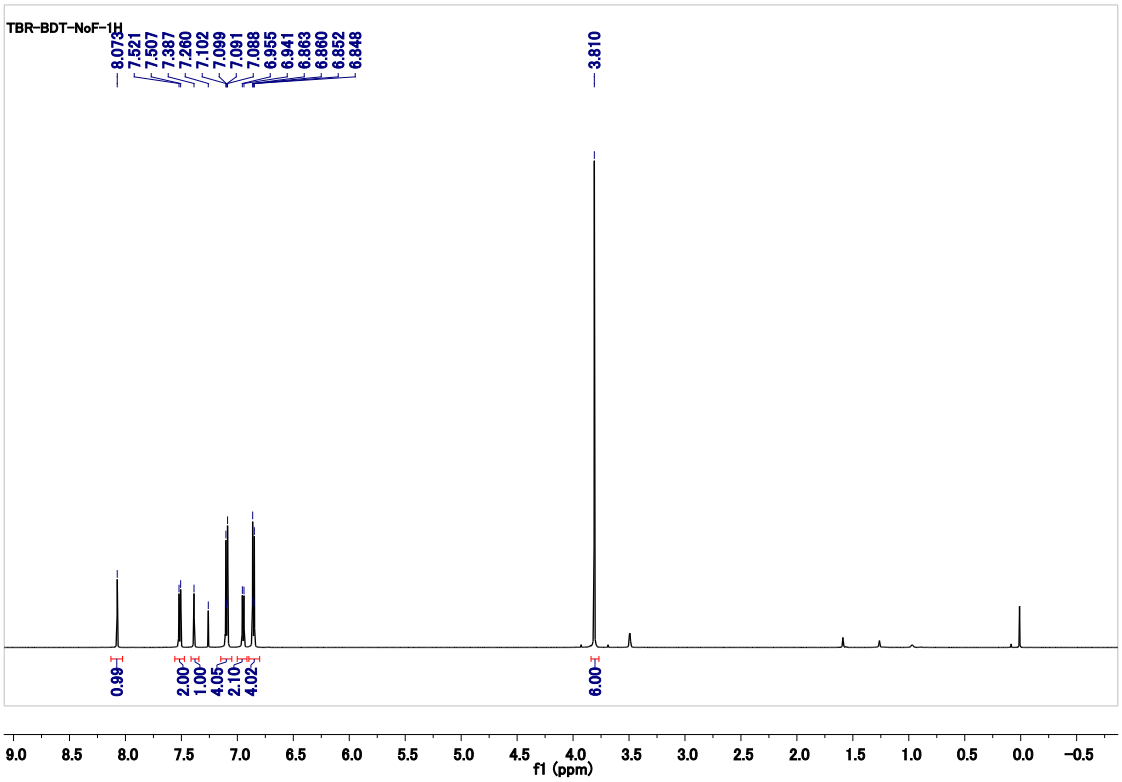

Fig. S10. ^{1}H NMR spectrum of compound 11 in deuterated chloroform.

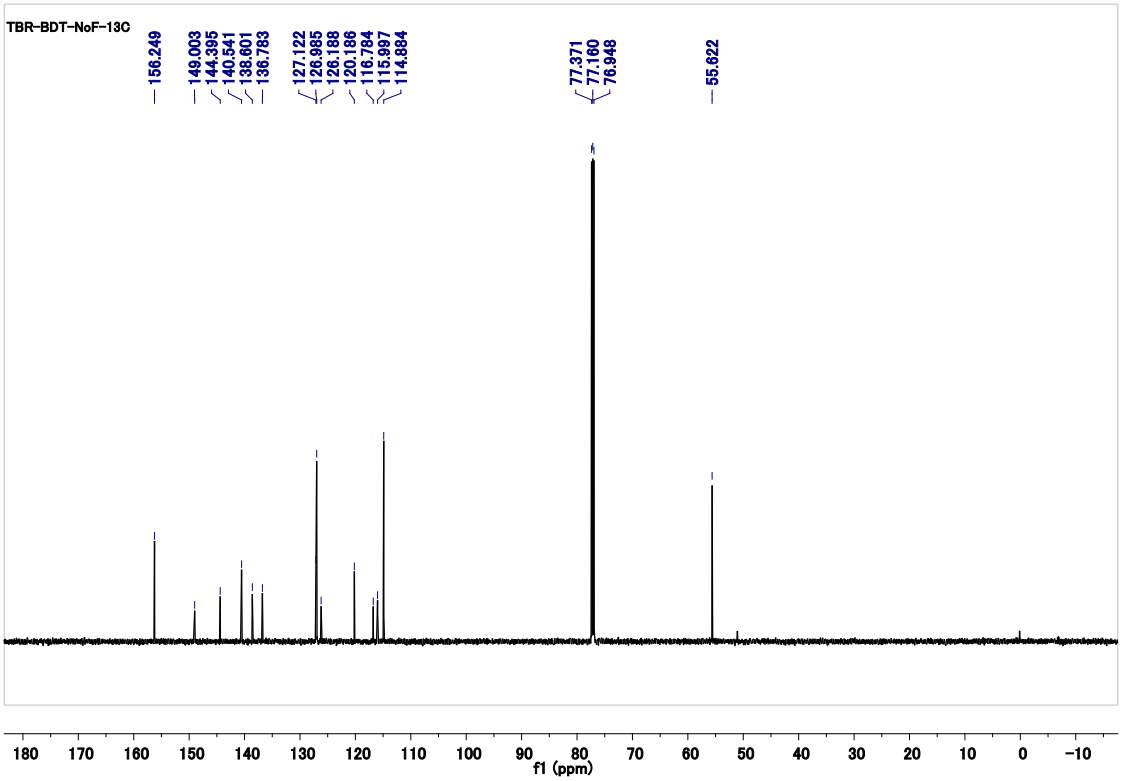

Fig. S11. ^{13}C NMR spectrum of compound 11 in deuterated chloroform.

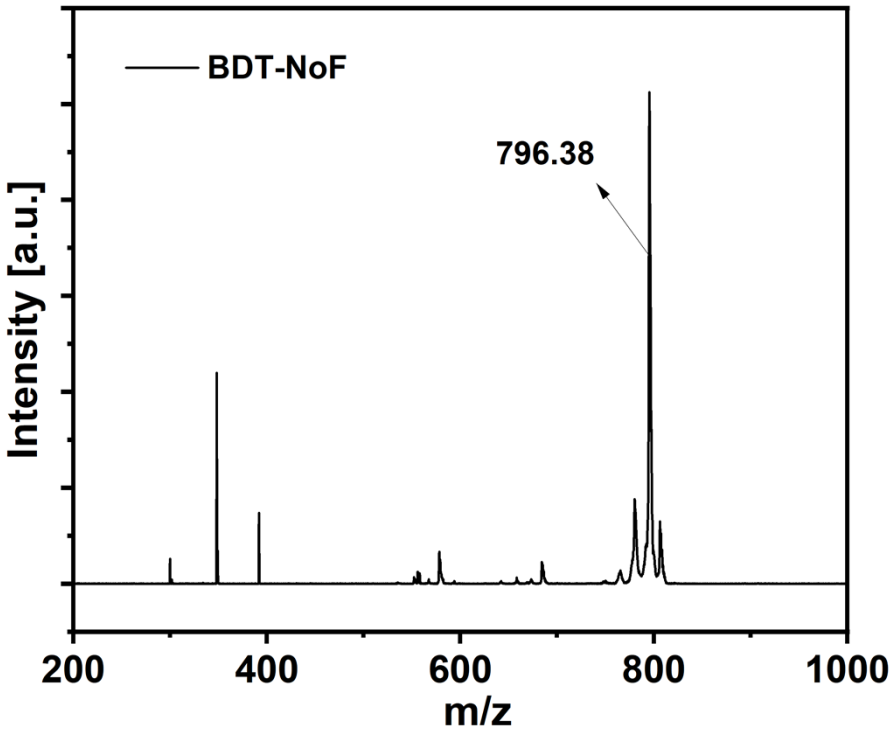

Fig. S12. Mass spectrum of compound 11.

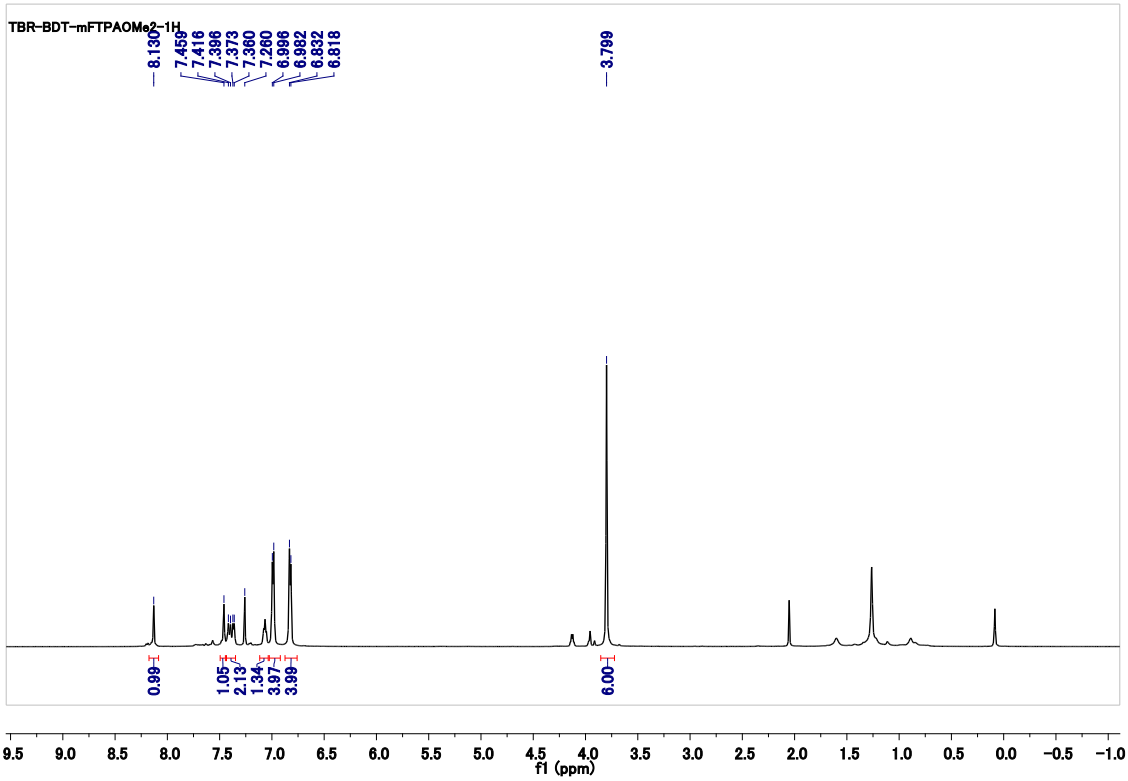

Fig. S13. ^{1}H NMR spectrum of compound 12 in deuterated chloroform.

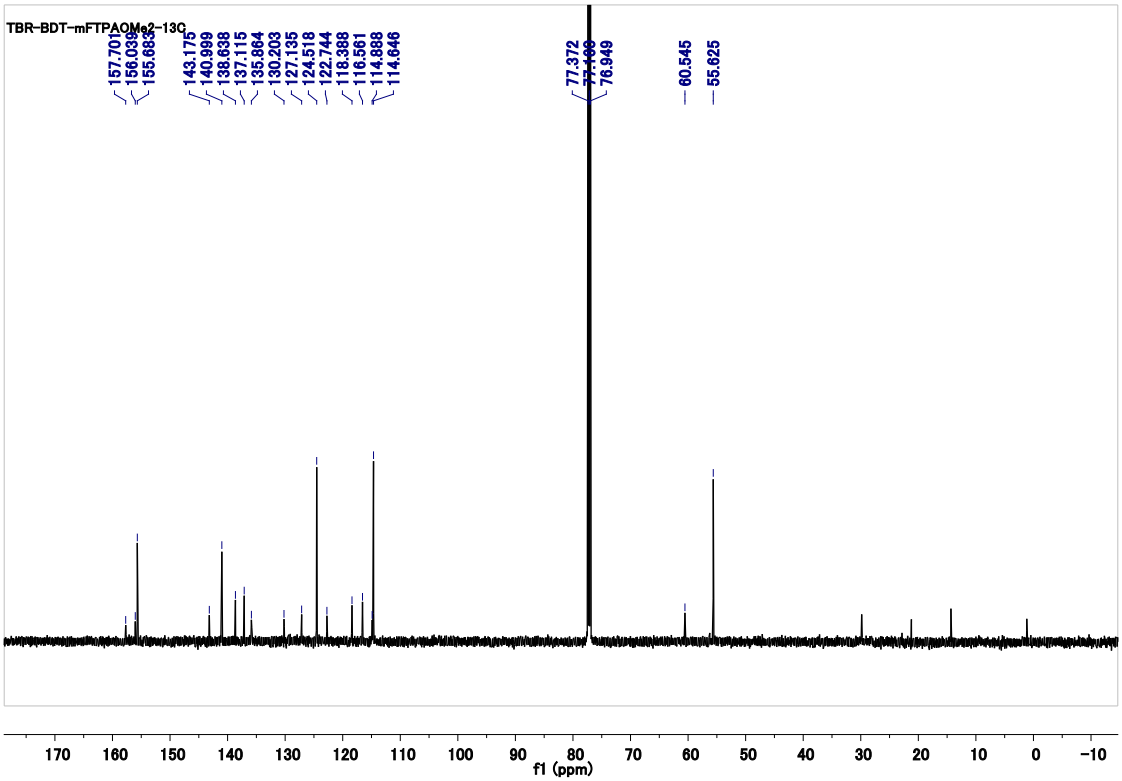

Fig. S14. ^{13}C NMR spectrum of compound 12 in deuterated chloroform.

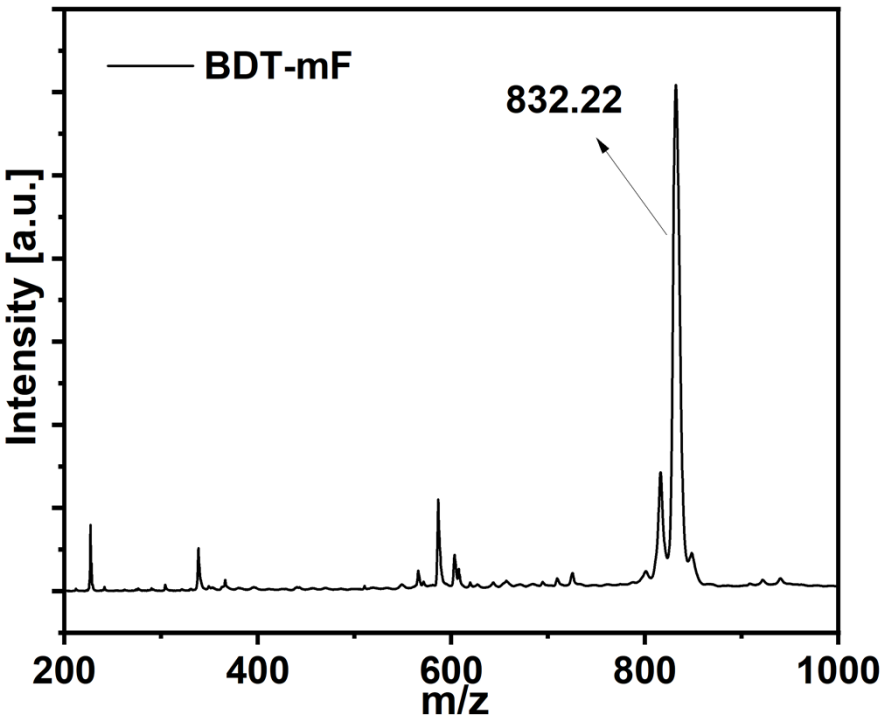

Fig. S15. Mass spectrum of compound 12.

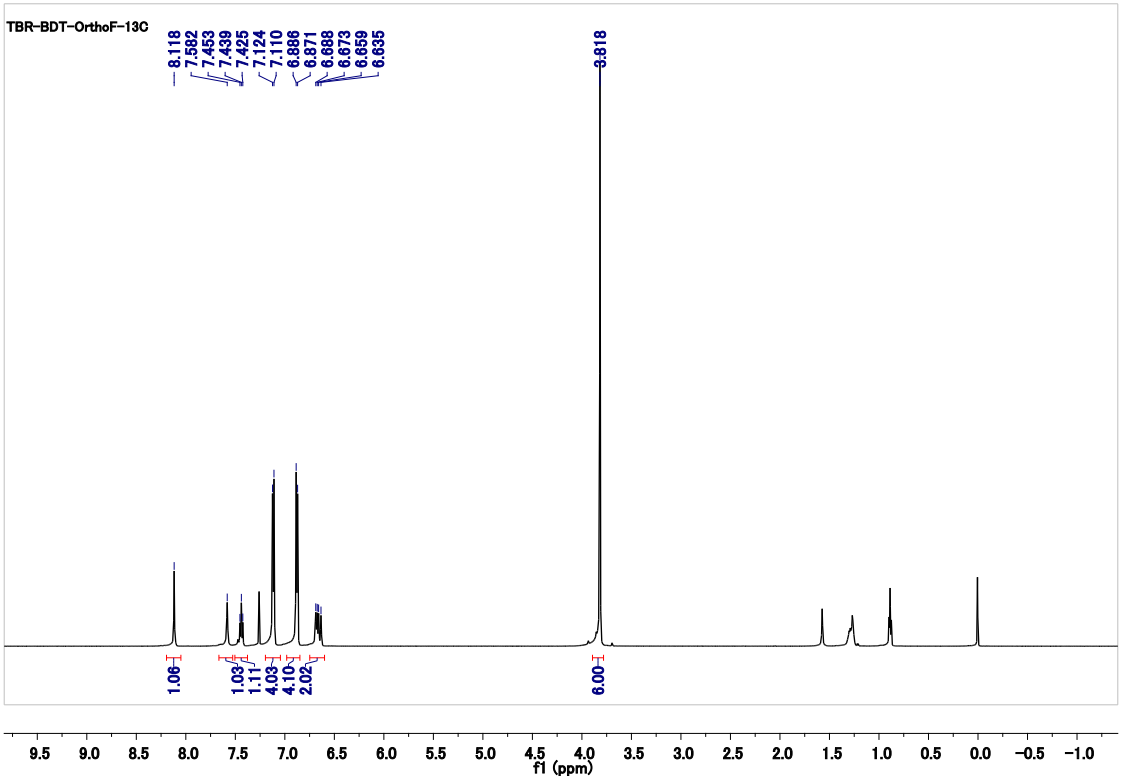

Fig. S16. ^{1}H NMR spectrum of compound 13 in deuterated chloroform.

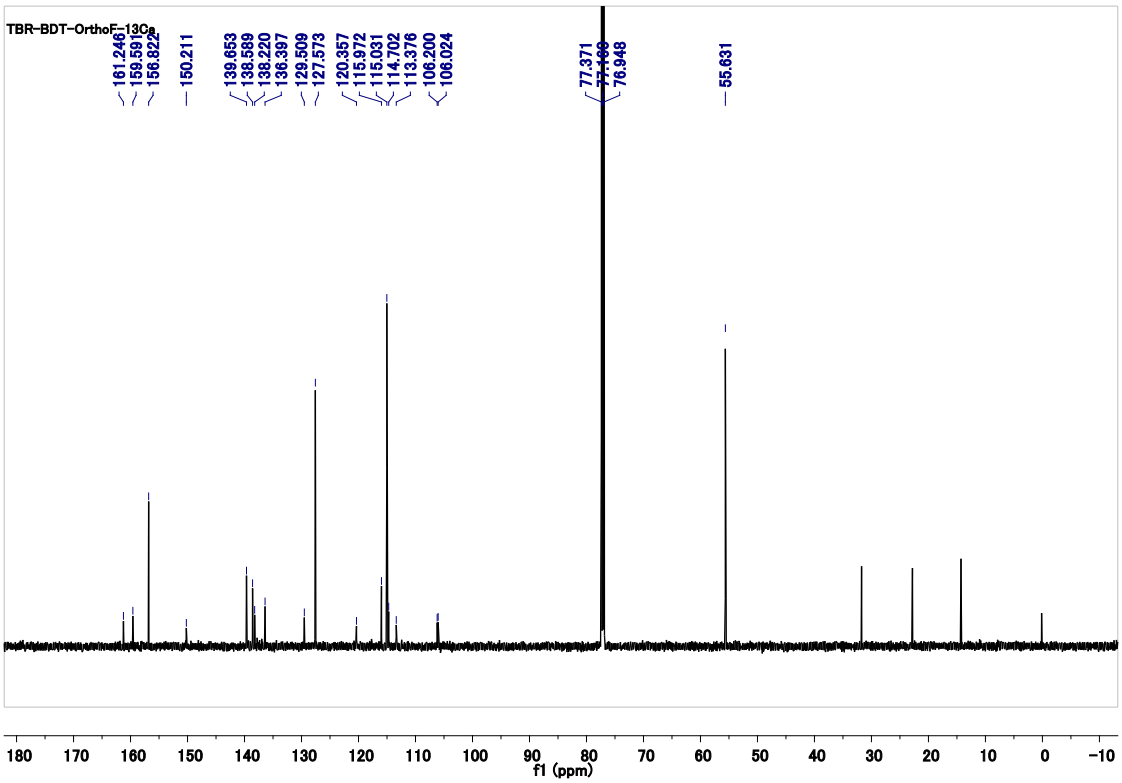

Fig. S17. ^{13}C NMR spectrum of compound 13 in deuterated chloroform.

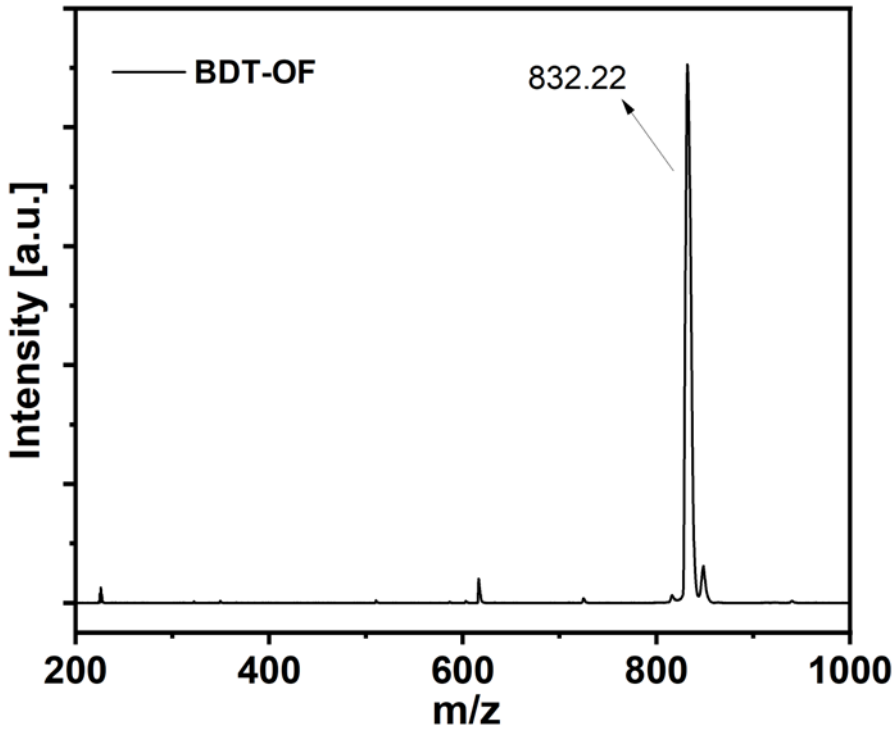

Fig. S18. Mass spectrum of compound 13.

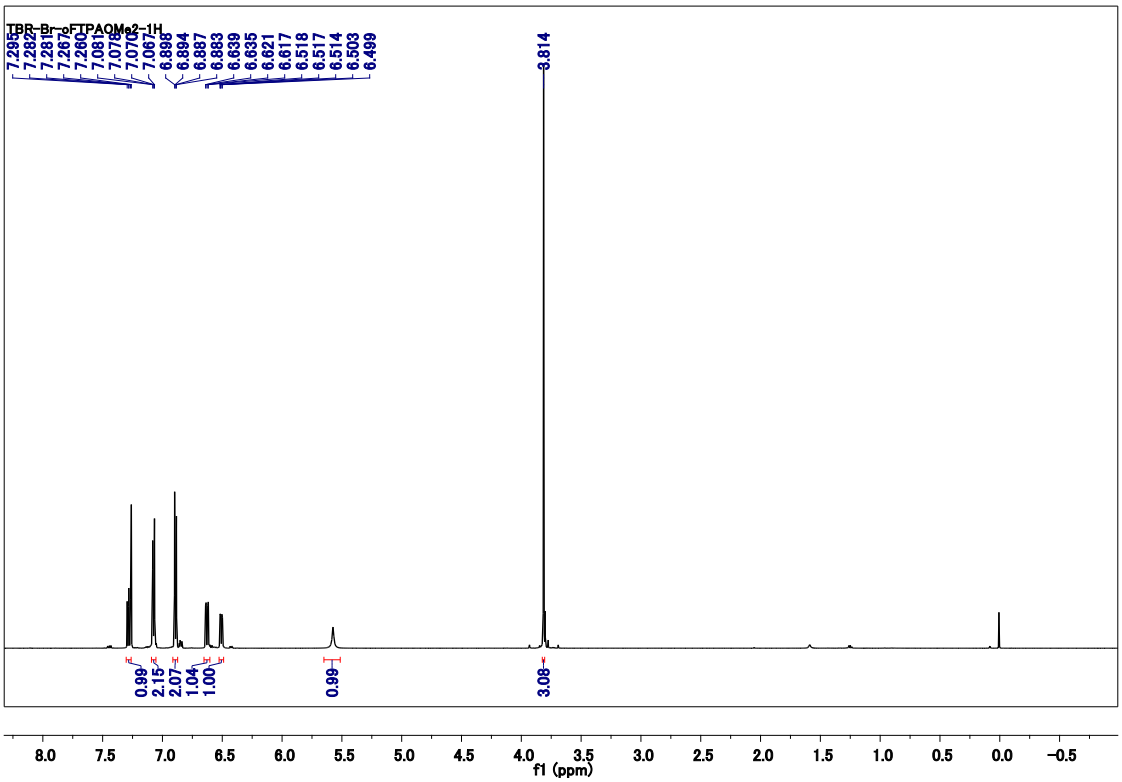

Fig. S19. ^{1}H NMR spectrum of compound 16 in deuterated chloroform.

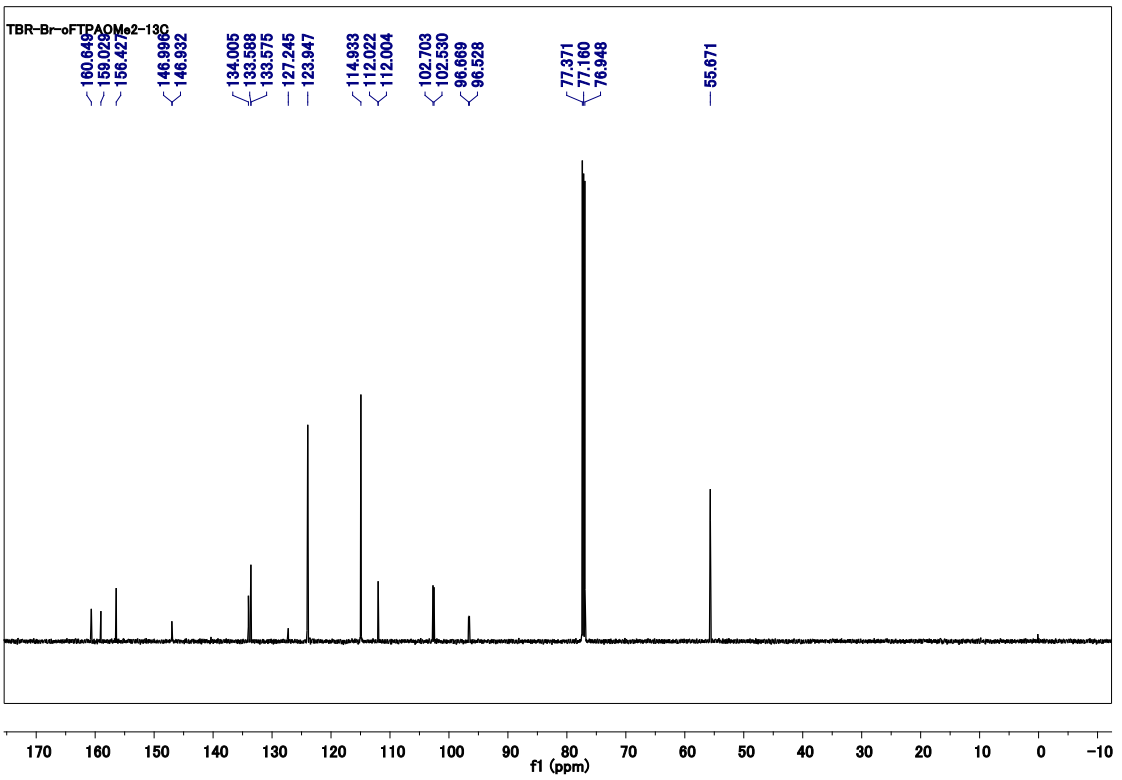

Fig. S20. ^{13}C NMR spectrum of compound 16 in deuterated chloroform.

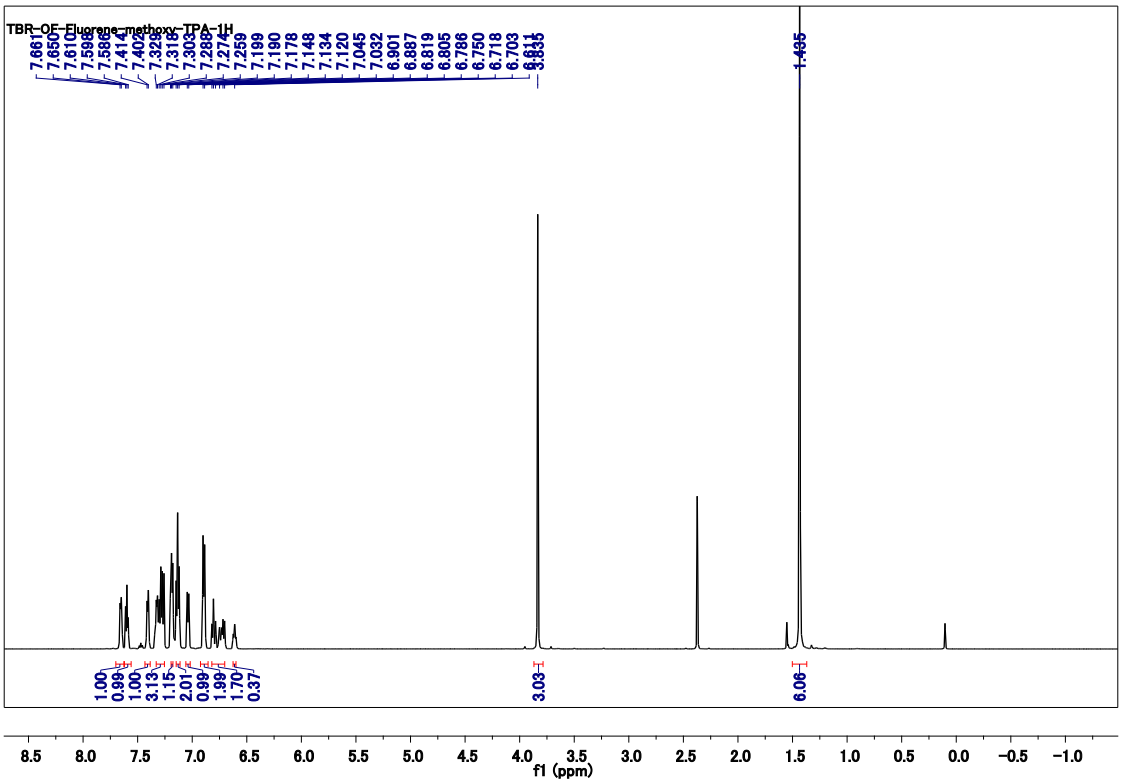

Fig. S21. [1]H NMR spectrum of compound 18 in deuterated chloroform.

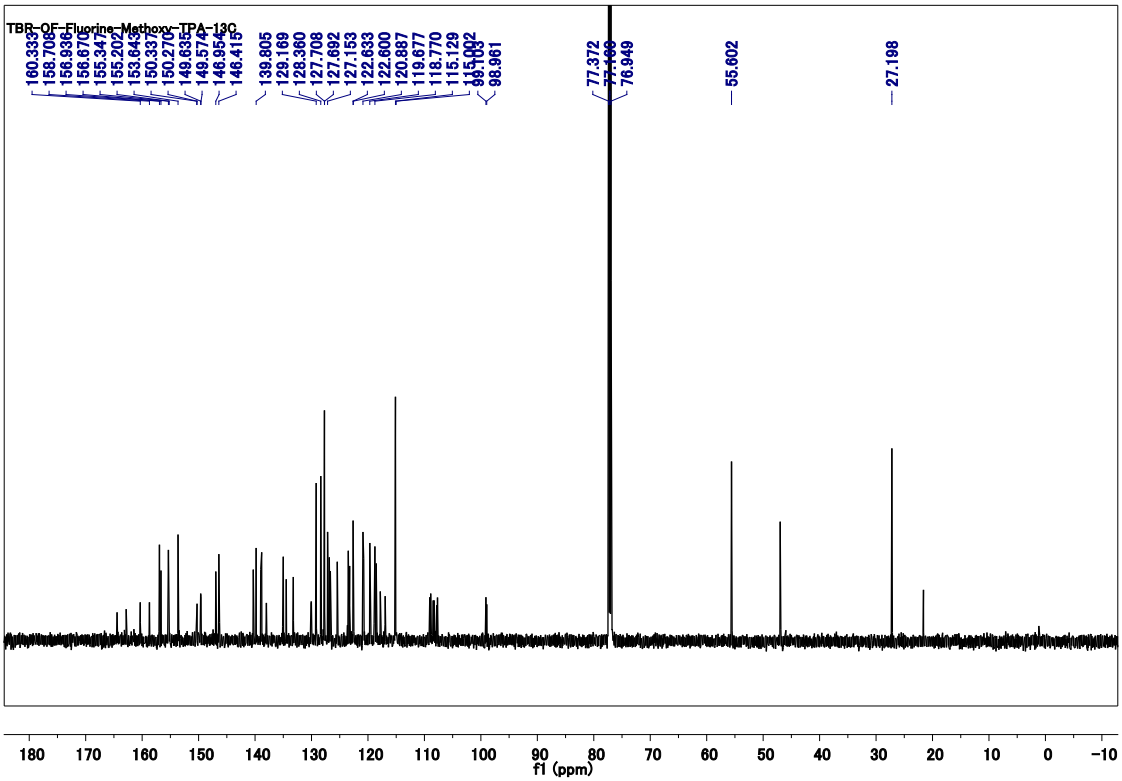

Fig. S22. [13]C NMR spectrum of compound 18 in deuterated chloroform.

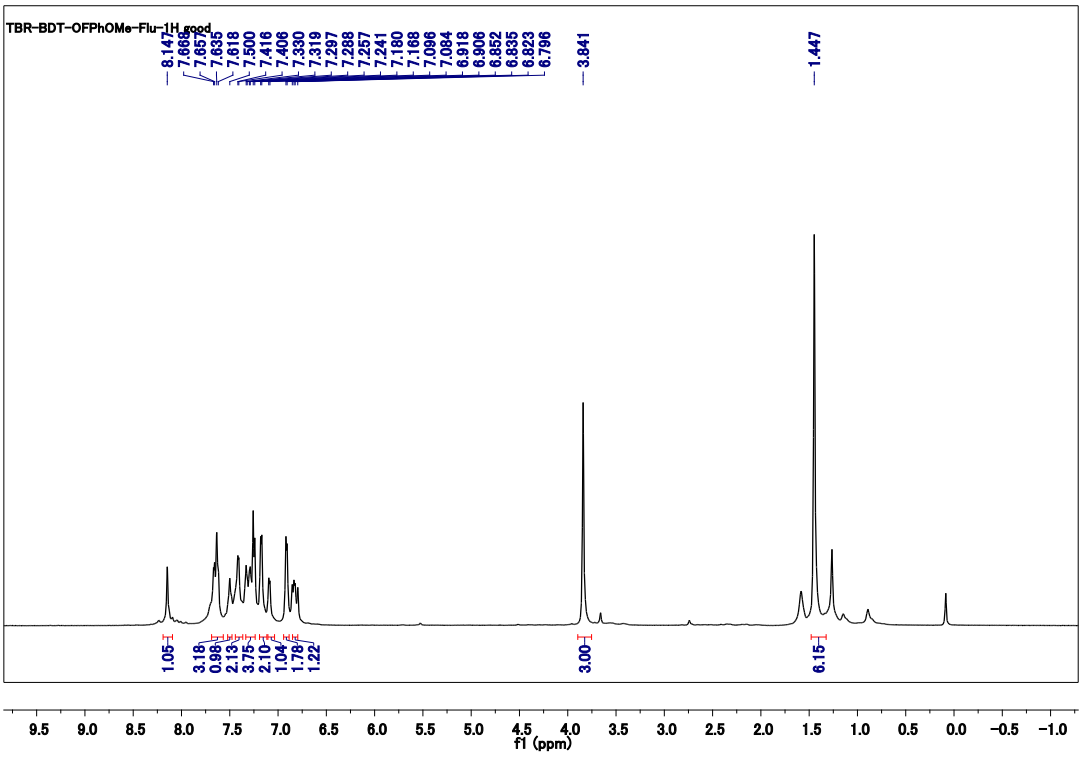

Fi

g. S23. ^{1}H NMR spectrum of compound 19 in deuterated chloroform.

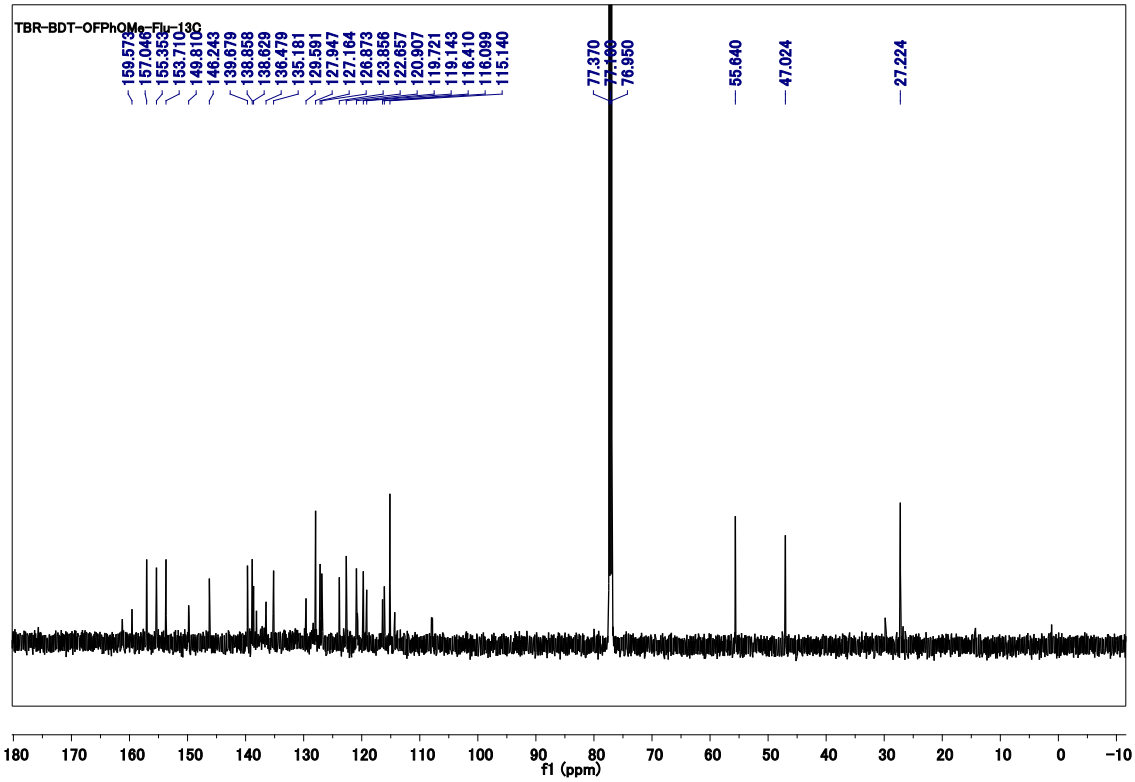

Fig. S24. ^{13}C NMR spectrum of compound 19 in deuterated chloroform.

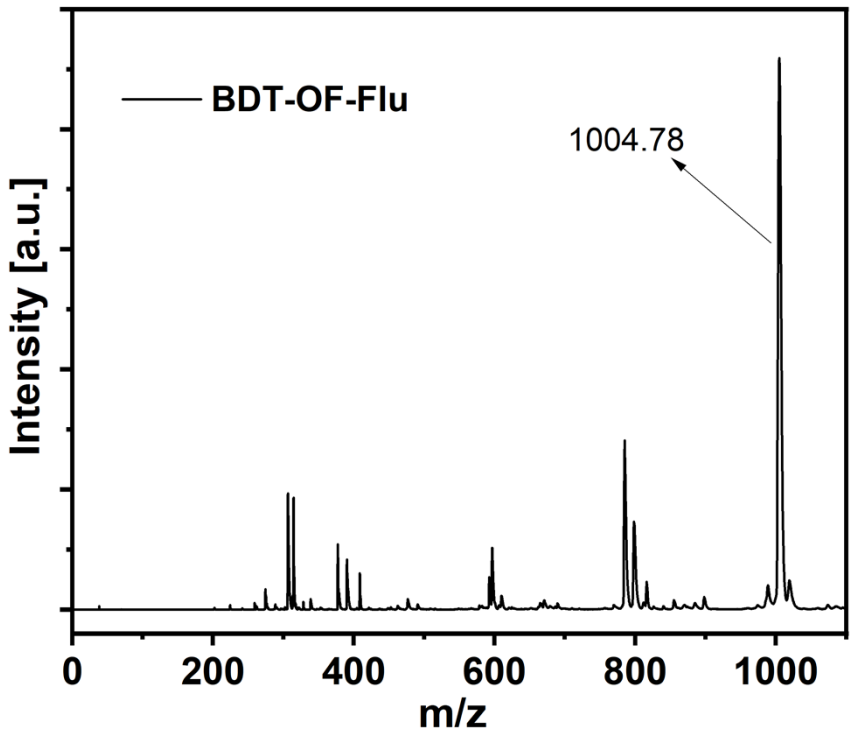

Fig. S25. Mass spectrum of compound 19.

2. Device Fabrication

2.1 Methods and materials

The SnO_2 colloidal solution (15% in H_2O colloidal dispersion) was purchased from Alfa Aesar. Formamidinium iodide (FAI), methylammonium bromide (MABr), lead iodide (PbI_2), lead bromide ($PbBr_2$), and cesium iodide (CsI) were obtained from Tokyo Chemical Industry. Chlorobenzene (CB), *N*,*N*-dimethylformamide (DMF), dimethyl sulfoxide (DMSO), acetonitrile,, 4-tert-butylpyridine (4-tBP), lithium bis(trifluoromethylsulfonyl)imide (LiTFSI), and tris(2-(1H-pyrazol-1-yl)-4-tert-butylpyridine)cobalt(III) tri[bis(trifluoromethanesulfonyl)imide] (FK-209) were purchased from Sigma-Aldrich. ITO-coated glass substrates were sourced from Atsugi Micro.

2.2 Preparation of precursor solutions:

A perovskite precursor solution was prepared by dissolving 1.10 M FAI, 0.20 M MABr, 1.15 M PbI_2, and 0.20 M $PbBr_2$ in an anhydrous DMF/DMSO solvent mixture (4:1 v/v). Additionally, a 0.08 M CsI solution in DMSO was added to the precursor mixture. The resulting solution was stirred at 70 °C for 1 hour and then filtered through a 0.2 μm polytetrafluoroethylene (PTFE) filter prior to use. Solutions of the HTMs were prepared by dissolving 30 mg of HTM in 0.5 mL CB. To this solution, 9 μL of LiTFSI solution (520 mg mL^{-1} in acetonitrile), 14.5 μL of FK-209 solution (300 mg mL^{-1} in acetonitrile), and 15 μL of 4-tert-butylpyridine (4-tBP) were added. All HTM precursor solutions were filtered through a 0.2 μm PTFE filter before use.

2.3 Fabrication of the devices:

Glass substrates with a pre-patterned ITO layer (~150 nm thick, Atsugi Micro) and a sheet resistance of ~10 Ω sq^{-1} were sequentially cleaned by ultrasonication in detergent, deionized water, acetone, and isopropanol for 10 minutes each. Prior to use, the cleaned ITO substrates were treated with UV–ozone for 15 minutes. A thin SnO_2 nanoparticle layer (SnO_2 colloid solution diluted 1:3 with deionized water) was spin-coated onto the ITO surface at 3000 rpm for 30 s, followed by annealing at 150 °C for 30 min. After cooling to room temperature, the SnO_2-coated substrates were subjected to a second UV–ozone treatment for 15 min. The perovskite layer was deposited using a two-step spin-coating process: 1000 rpm for 10 sec and then 6000 rpm for 30 sec. Ten seconds before the end of the spin-coating, 140 μL of CB was dropped onto the spinning substrate. The films were then immediately annealed on a hot plate at 100 °C for 30 min. Next, the synthesized HTM was spin-coated onto the perovskite layer at 4000 rpm for 30 sec.

Finally, an ~80 nm Au electrode was thermally evaporated under a base pressure of 10^{-4} Pa with a deposition rate of ~0.1 nm s^{-1}.

2.4 Solar cell performance measurement

All *J–V* curves in this study were recorded using a computer-controlled Keysight B2901A source/measure unit under simulated AM1.5G solar illumination from a Xe lamp-based solar simulator (HAL-320, Asahi Spectra). Measurements were performed in the backward scan direction with a scan rate of 200 mV s^{-1}, while the voltage sweep rate was maintained at 0.05 V s^{-1}. The original PSC area, defined by the overlap of the ITO and Au electrodes, was 0.04 cm^2, whereas the illumination area during *J–V* measurements was precisely set to 0.0369 cm^2 (determined via optical microscopy) using a black shadow mask. The lamp power was carefully calibrated to 100 mW cm^{-2} using a crystalline Si reference cell with an amorphous Si optical filter (Bunko-Keiki), certified by the National Institute of Advanced Industrial Science and Technology of Japan. IPCE measurements of the PSCs were conducted using a Keysight B2901A source/measure unit coupled with a constant-energy monochromatic light source (PVL-5000, Asahi Spectra). The optical power of the monochromatic light was quantified using a power meter (843-R, Newport) in combination with an optical power detector (818-UV/DB, Newport) to enable accurate IPCE calculation. For electrical characterization, devices with the structure glass substrate/ITO (≈100 nm)/chemically doped HTM layer/MoO_3 (10 nm)/Al (≈100 nm) were fabricated, and their *J–V* characteristics were measured in the dark using a computer-controlled Keithley 2400 source unit. The electrical conductivity of the HTM layers was extracted from the slope of the *J–V* curves.

Table S1. Device results of BDT-NoF-based PSCs.

Cell	J_{SC} (mA cm^{-2})	V_{OC} (V)	FF	PCE (%)
1	22.5587	0.99627	0.63495	14.2702
2	22.8553	0.99988	0.63475	14.5057
3	22.5823	0.98061	0.62509	13.8423
4	22.704	0.98733	0.6055	13.5731
5	22.012	0.97985	0.63414	13.6775
6	22.1407	1.04215	0.66436	15.3295
7	22.0621	1.07628	0.66774	15.8555
8	22.9314	1.03047	0.68072	16.0854
9	23.1341	1.00534	0.68871	16.0179
10	22.4697	0.98043	0.67593	14.8907
11	23.4882	0.98548	0.68447	15.8436
12	23.294	0.9974	0.66861	15.5342

Table S2. Device results of BDT-mF-based PSCs.

Cell	J_{SC} (mA cm^{-2})	V_{OC} (V)	FF	PCE (%)
1	22.506	0.91601	0.61504	12.6794
2	22.5618	0.89878	0.61147	12.3994
3	22.1723	0.90358	0.60754	12.1718
4	22.3587	0.89213	0.55316	11.0338
5	23.3575	0.91568	0.59399	12.7044
6	23.4322	0.90285	0.59003	12.4826
7	23.2183	0.90868	0.59483	12.5498
8	23.2134	0.89443	0.59117	12.2744
9	23.4026	0.89939	0.59695	12.5645
10	23.3727	0.89672	0.59898	12.554
11	23.5808	0.90986	0.61249	13.1411
12	23.3881	0.90567	0.6053	12.8214

Table S3. Device results of BDT-OF-based PSCs.

Cell	J_{SC} (mA cm^{-2})	V_{OC} (V)	FF	PCE (%)
1	23.0138	0.99787	0.71828	16.4953
2	23.2084	1.00257	0.70208	16.3361
3	23.3338	1.01722	0.68789	16.3276
4	23.8549	1.00925	0.72492	17.4528
5	23.3067	1.04009	0.69562	16.8626
6	23.3589	1.03176	0.67993	16.3869
7	23.613	1.03512	0.68116	16.6491
8	23.2663	1.03877	0.70022	16.9231
9	22.505	1.03193	0.74978	17.4126
10	22.674	1.0091	0.73689	16.8602
11	22.7596	1.01792	0.7437	17.2295
12	23.4288	1.01922	0.67704	16.1671

Table S4. Device results of BDT-OF-Flu-based PSCs.

Cell	J_{SC} (mA cm^{-2})	V_{OC} (V)	FF	PCE (%)
1	24.0334	0.91087	0.35046	7.6719
2	23.775	0.88028	0.40515	8.4792
3	24.8157	0.85979	0.34846	7.4348
4	24.5052	0.85627	0.37856	7.9434
5	23.6288	0.90548	0.43859	9.3837
6	23.1194	0.89367	0.43618	9.012
7	22.9114	0.87204	0.45958	9.1822
8	23.6186	0.82958	0.37606	7.3684
9	23.6413	0.86836	0.34367	7.0553
10	23.6186	0.82958	0.37606	7.3684
11	24.0341	0.96809	0.33279	7.743

Table S5. Device results of spiro-OMeTAD-based PSCs.

Cell	J_{SC} (mA cm^{-2})	V_{OC} (V)	FF	PCE (%)
1	22.9984	1.1165	0.76305	19.593
2	23.0868	1.1096	0.76126	19.502
3	22.8045	1.1115	0.76641	19.427
4	22.7408	1.1062	0.76936	19.354
5	22.7348	1.1076	0.75291	18.960
6	22.9088	1.1031	0.74796	18.902
7	23.2912	1.0903	0.73717	18.720
8	23.2317	1.0976	0.74941	19.110
9	24.0104	1.0894	0.72748	19.028
10	24.0111	1.0981	0.75595	19.932
11	23.8404	1.0963	0.74773	19.544
12	22.7354	1.1329	0.74839	19.2762

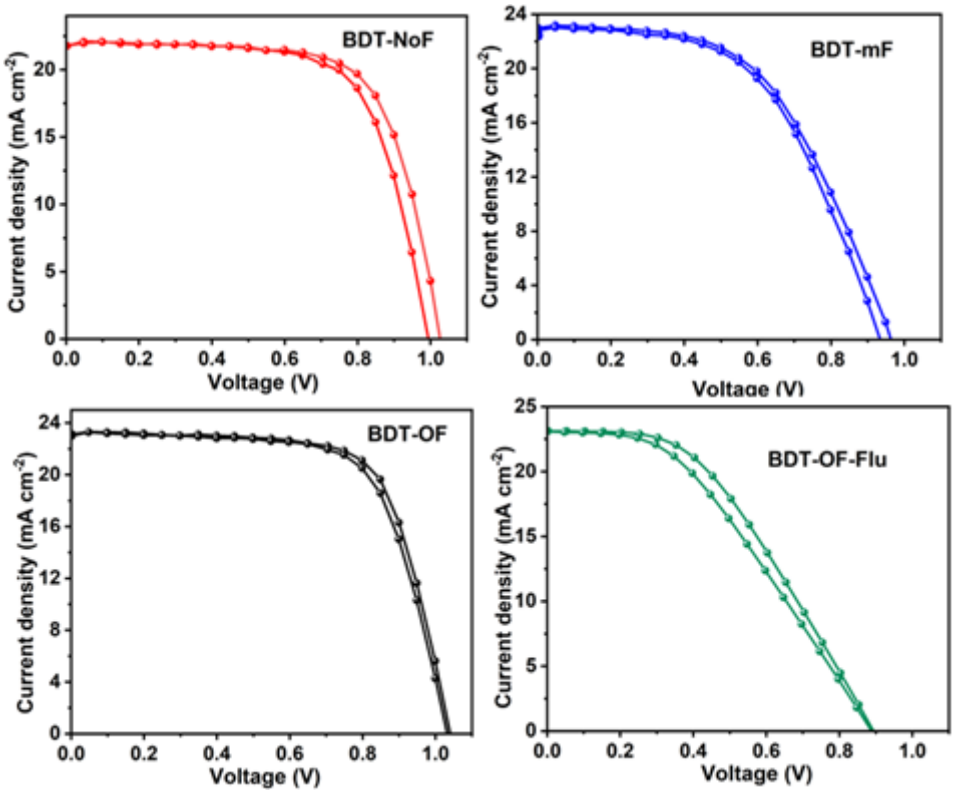

Fig. S26. Forward and reverse *J*–*V* curves of PSCs.

Table S6. Device results of PSCs. The hysteresis index (HI) was calculated from the following equation: HI = 100 × (PCE_F–PCE_R)/PCE_F.

HTM	Device	J_{SC} (mA cm^{-2})	V_{OC} (V)	FF	PCE (%)	HI
BDT-NoF	Forward	22.14	1.04	0.66	15.32	1.95
	Reverse	22.10	0.99	0.68	15.02	
BDT-mF	Forward	23.43	0.90	0.59	12.48	1.76
	Reverse	23.30	0.89	0.59	12.26	
BDT-OF	Forward	23.30	1.04	0.69	16.86	2.8
	Reverse	23.34	1.03	0.67	16.38	
BDT-OF-Flu	Forward	23.11	0.89	0.43	9.01	8.9
	Reverse	23.09	0.89	0.40	8.2	

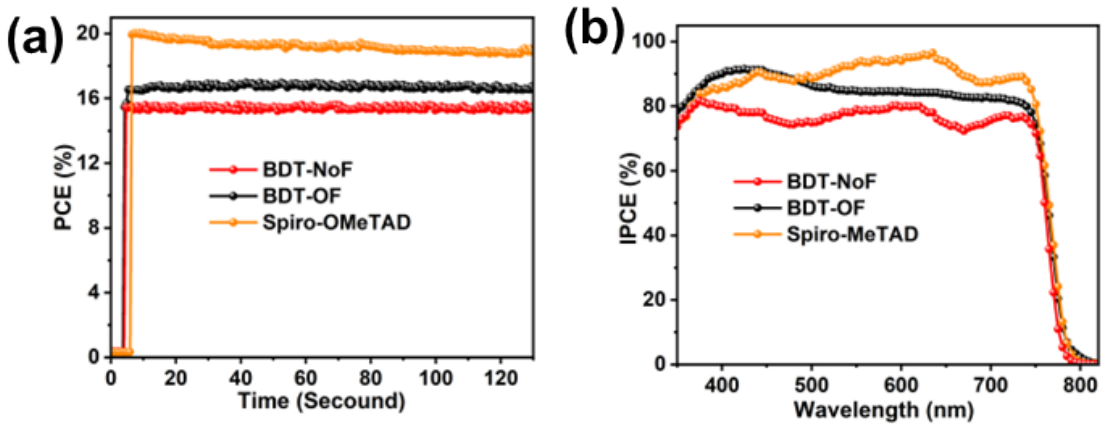

Fig. S27. (a) PCE tracking results and (b) IPCE curves of PSCs based on BDT-NoF, BDT-OF, and spiro-OMeTAD.

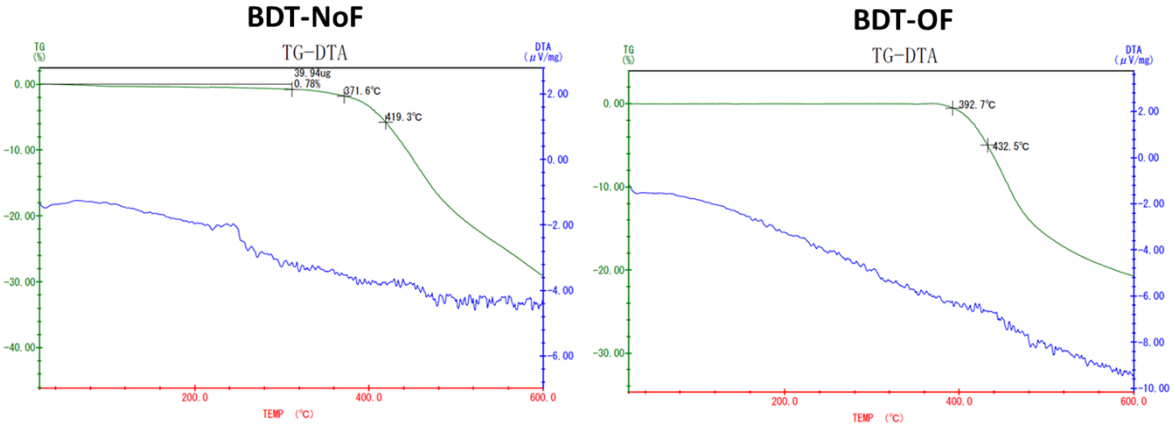

Fig. S28. TG-DTA results of BDT-NoF and BDT-OF.

References

S1. N. M. Patil, A. A. Kelkar, Raghunath V. Chaudhari. *J. M. Cat. A: Chem*.C, 2004, **223,** 45–50.

S2. T B. Raju, C. A. M. Senevirathne, M. Watanabe, Y. Fujita, D. Senba and T. Matsushima, *J. Mater. Chem. C,* 2025, **13**, 15082-15090.

S3. M. Zhai, N. Shibayama, T. B. Raju, T. Wu, C. Chen, Z. Guo, T. Matsushima, T. Miyasaka and M. Cheng, *Small* **2025**, 2505961.

S4. H. Zhang, X. Yu, M. Li, Z. Zhang, Z. Song, X. Zong, G. Duan, W. Zhang, C. Chen, W. H. Zhang, Y. Liu and M. Liang, *Angew. Chem. Int. Ed.,* 2023, **62**, e202314270.